

UPDATE IN RADIOLOGY

Functional imaging in pancreatic disease[☆]



S. Baleato-González^{a,*}, R. García-Figueiras^a, A. Luna^b,
M. Domínguez-Robla^a, J.C. Vilanova^c

^a Departamento de Radiología, Complejo Hospitalario Universitario de Santiago de Compostela, Santiago de Compostela, A Coruña, Spain

^b Grupo Health Time, Director – Advanced Medical Imaging, Sercosa (Servicio de Radiología Computerizada), Clínica Las Nieves, Jaén, Spain

^c Departamento de Radiología, Clínica Girona-Hospital Santa Caterina, Girona, Spain

Received 30 January 2018; accepted 23 July 2018

KEYWORDS

Pancreas;
Magnetic resonance
imaging;
Diffusion;
Dual-energy
computed
tomography;
Perfusion;
Cholangiography

Abstract In addition to the classical morphological evaluation of pancreatic disease, the constant technological advances in imaging techniques based fundamentally on computed tomography and magnetic resonance imaging have enabled the quantitative functional and molecular evaluation of this organ. In many cases, this imaging-based information results in substantial changes to patient management and can be a fundamental tool for the development of biomarkers. The aim of this article is to review the role of emerging functional and molecular techniques based on computed tomography and magnetic resonance imaging in the evaluation of pancreatic disease.

© 2018 SERAM. Published by Elsevier España, S.L.U. All rights reserved.

PALABRAS CLAVE

Páncreas;
Resonancia
magnética;
Difusión;
TC de energía dual;
Perfusión;
Colangiografía

Imagen funcional de la patología pancreática

Resumen El constante avance tecnológico de las técnicas de imagen basadas fundamentalmente en la tomografía computarizada y la resonancia magnética ha permitido, además de la clásica valoración morfológica de la patología pancreática, su evaluación cuantitativa funcional y molecular. Esta información basada en la imagen conlleva en muchos casos un sustancial cambio en el manejo de los pacientes y podría ser una herramienta fundamental en el desarrollo de biomarcadores. El objetivo de este artículo es revisar el papel de las técnicas emergentes funcionales y moleculares basadas en la tomografía computarizada y la resonancia magnética, para la valoración de la patología pancreática.

© 2018 SERAM. Publicado por Elsevier España, S.L.U. Todos los derechos reservados.

[☆] Please cite this article as: Baleato-González S, García-Figueiras R, Luna A, Domínguez-Robla M, Vilanova JC. Imagen funcional de la patología pancreática. Radiología. 2018;60:451–464.

* Corresponding author.

E-mail address: baleatorum@hotmail.com (S. Baleato-González).

Introduction

Radiological images have evolved from the anatomical setting to the possibility of evaluating the functional and molecular characteristics of tissues. The development of multiple advanced imaging modalities fundamentally based on computed tomography (CT) scans and magnetic resonance imaging (MRI) has changed the way we approach and manage pancreatic disease. These techniques provide a better capacity of detection and characterization and play a significant role in the therapeutic decision-making process and management of patients. This paper will review their actual clinical applications and limitations.

Advanced computed tomography imaging modalities

Dual-energy computed tomography imaging

The dual-energy computed tomography (DECT) imaging modality consists of the acquisition of images by combining different kilovoltages (the most commonly used are 80 kV and 140 kV). Since the absorption of x-rays depends on the energy of the beam and the attenuation of several chemical elements is different at 80 kV than it is at 140 kV, we can classify them by analyzing the difference of attenuation with respect to each spectrum of energy. Also, the iodine of one CT scan conducted with a contrast agent can be subtracted to obtain the so-called studies "without virtual contrast" or else to generate "iodine distribution maps", and also conduct iodine quantification studies (Fig. 1). The DECT provides better pancreatic adenocarcinoma detection. Several authors have demonstrated that the use of low kilovoltages (80 kV) allows us to better differentiate between tumor and normal pancreatic tissue.^{1,2} Another study that compared the multiphase CT scan to the DECT showed higher diagnostic sensitivity with the use of dual energy.³ Similarly, recent studies have shown promising findings distinguishing adenocarcinomas from chronic pancreatitis-induced inflammatory mass with the use of dual energy.⁴

Also, the DECT allows us to conduct pancreatic studies with lower doses of radiation since we can suppress the phase without contrast thanks to the "CT scan without virtual contrast" and thus minimize the dose of iodinated contrast used given its higher intrinsic contrast thanks to the use of low kilovoltages.⁵ In patients with acute pancreatitis, Wichmann et al. showed that one single portal phase with the DECT imaging modality would be enough to assess the index of severity, meaning that it is possible to suppress the phase without contrast and the arterial phase, thus limiting the dose of radiation used.⁶

Another new field of study is virtual cholangiography, but very few studies have been published to date that assess the use of the DECT imaging modality to determine the composition of biliary lithiasis.⁷

Computed tomography perfusion imaging

The computed tomography perfusion (CTP) imaging is one functional technique that allows us to study the vascularization characteristics of a given organ. This technique is based on monitoring the passage of contrast through the vascular bed with a linear correlation between the concentration of contrast and attenuation. To conduct this imaging modality, serial quick slices are acquired on the same region after the administration of high flow endovenous contrast to obtain temporal information on the passage of contrast through the network of capillaries. Depending on the mathematical model used, it is possible to estimate the quantitative maps of different parameters including the blood flow (BF), the blood volume (BV), the mean transit time (MTT), or the transfer coefficient (K^{trans}) for the functional study of tissue vascularization.⁸

Mostly the CTP has been used in the pancreas for the assessment of tumors and inflammatory disease. In the field of oncology, the CTP is a non-invasive way to study the phenomenon of tumor angiogenesis.⁹ In general, tumors here show an increased vascularization and impaired patency (Fig. 2). In the case of pancreatic adenocarcinomas, we should consider the extensive desmoplastic reaction associated, which would explain its lower perfusion compared to pancreatic parenchyma. The CTP has proven useful in the diagnosis, staging, and prognosis of patients with neuroendocrine tumors (NET) since it is associated with their degree of aggressiveness. These tumors show higher parameters of BV and BF compared to a normal pancreas.¹⁰⁻¹² Zhu et al. confirmed that when the CTP is combined with conventional imaging techniques, it increases the diagnostic performance of insulinomas.¹³ On the other hand, the degree of tumor differentiation of adenocarcinomas seems to be associated with the BV. Thus, high-grade adenocarcinomas show lower BV and lower values of enhancement peak.¹⁴

Also, perfusion allows us to assess the response of the tumor to different therapies. It has been reported that tumors with higher values of K^{trans} usually show better response to radiochemotherapy¹⁵ and that, when it comes to antiangiogenic therapy, higher basal values of BF and BV associate better responses to such therapy. It can also be a useful tool to assess the early response of NET after confirming the drop of BF 48 h after initiating antiangiogenic therapy and then the drop of BV (Fig. 3).^{15,16}

Another interesting aspect here is the possible use of the CTP to differentiate chronic pancreatitis-induced inflammatory masses from adenocarcinomas. Both entities would show lower perfusion compared to a normal parenchyma, but this decrease would be higher if dealing with cancer.^{10,11} This imaging modality can also be used to diagnose isodense tumors with parenchyma in the study of conventional CT scans.¹¹

In the case of pancreatic inflammatory disease, several authors have studied the role that the CTP plays in the diagnosis of acute or chronic pancreatitis and in the early prediction of developing necrosis in acute pancreatitis.^{8,17,18} Pieńkowska et al. suggest that the CTP

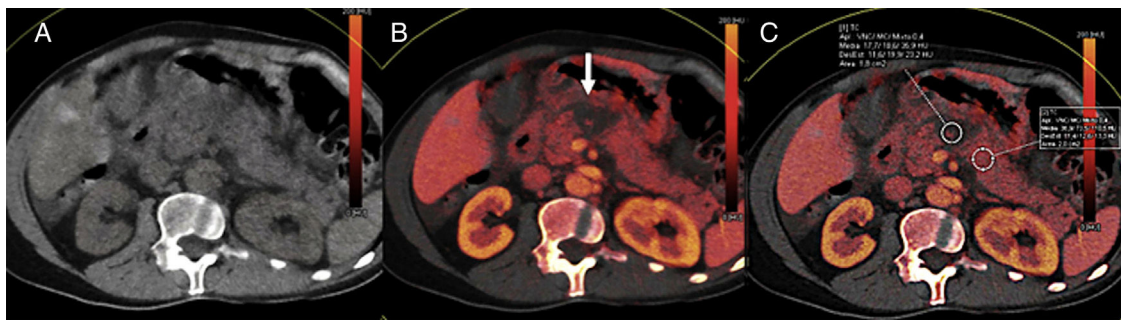


Figure 1 55-year-old male with acute pancreatitis. Computed tomography (CT) scan without contrast (A), color-coded iodine concentration map (B) and map with region of interest (ROI) measuring the concentration of iodine (C). The dual-energy computed tomography shows an area of necrosis at the level of the pancreatic body shown in the color-coded iodine concentration map as an area without iodinated contrast uptake (arrow) being the iodine quantified by placing one ROI in the gland parenchyma.

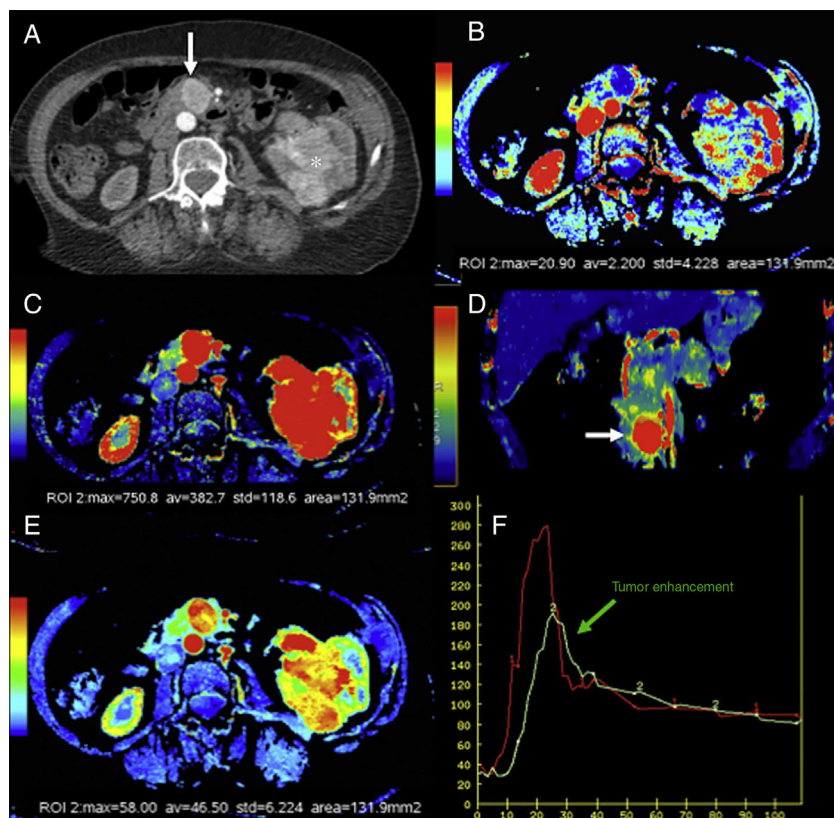


Figure 2 Computed tomography (CT) scan with perfusion in a patient with clear cell carcinoma in left kidney and metastasis in the pancreatic uncinate (arrows). CT scan with contrast in the arterial phase (A), parametric maps in the axial plane of patency (B) of blood flow in the axial (C) and coronal (D) planes and of blood volume (E) and uptake curves of aorta and tumor (F). The color-coded maps show high values of blood flow and volume and low values of patency in the pancreatic metastatic lesion compared to a normal pancreas. The imaging time-curve-type analysis shows an enhanced pancreatic metastasis (green curve) with a similar morphology to that of the aorta (red curve).

could also be used to select, during the first 24 h following symptom onset, patients at risk of developing pancreatic or peripancreatic necrosis.¹⁹ The group led by Yadav showed that the following cut-off points for the BF and the BV (27.29 ml/100 ml/min and 8.96 ml/100 ml,

respectively) facilitated predicting the presence of necrosis with 87.5% sensitivity and 100% specificity.¹⁷ In the case of chronic pancreatitis, the possible utility of perfusion in its early diagnosis has also been suggested.^{8,10,20}

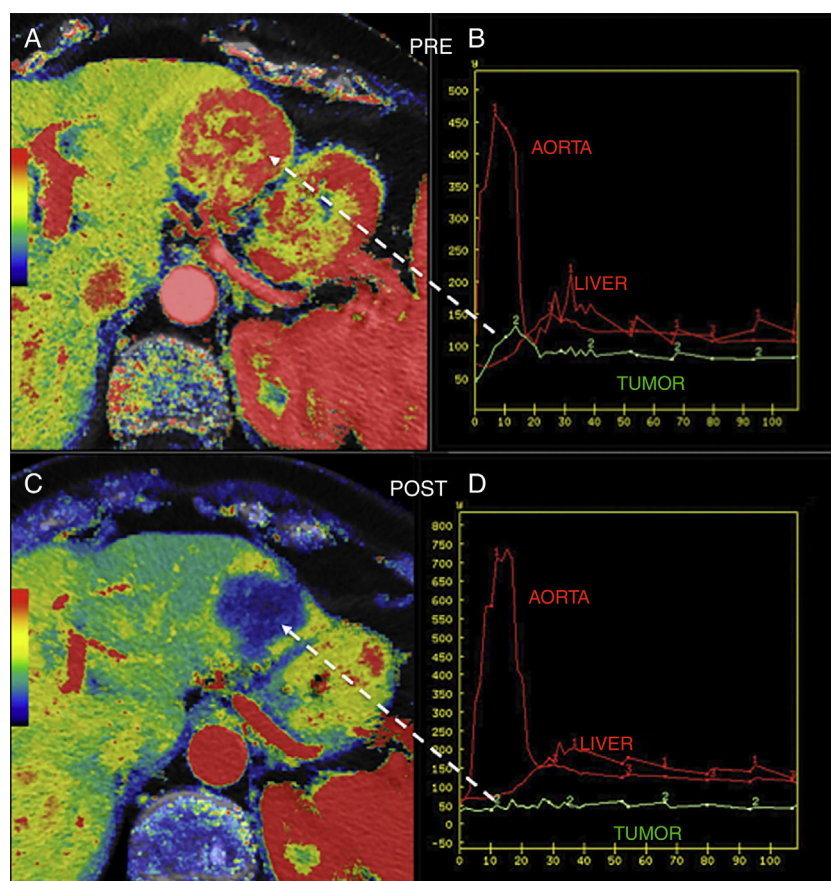


Figure 3 Hepatic metastasis of pancreatic neuroendocrine tumor treated with antiangiogenic therapy. Parametric maps of blood flow pre-treatment (A) and 15 days after angiogenic therapy (C) overlapping the anatomical image of a CT scan (50% transparency) and uptake curves of the metastatic lesion (in green), the aorta and the normal hepatic parenchyma (B and D) showing significant tumor response with a drop of metastatic flow from 118 ml/100 g/min to 8 ml/100 g/min and change in the morphology of the enhancement curve of the lesion from one enhancement curve with washout (type 3) (B) to one plane curve with almost no changes (D).

Advanced magnetic resonance imaging

Secretin-enhanced magnetic resonance cholangiopancreatography

The magnetic resonance cholangiopancreatography (MRCP) evaluates the pancreatic and biliary ductal morphology thanks to the use of heavily T2-weighted sequences that show the fluid content of biliopancreatic ducts, but the adjacent tissues are suppressed in the image. Secretin is one hormone that stimulates the secretion of water and bicarbonate through the pancreatic ductal cells and elevates the sphincter of Oddi tone during the first 5–6 min after its administration. As a result, it increases the fluid content inside the pancreatic ducts and, consequently, their size. The secretin-enhanced MRCP plays an important role in the diagnosis of ductal anatomical variants, complications such as pancreatic duct disruption (Fig. 4), or functional disorders such as disruptions in the sphincter of Oddi. Also, with the MRCP we can conduct early diagnoses of chronic

pancreatitis because it provides us with better visualization of the main pancreatic duct and its secondary branches and estimates the exocrine pancreatic function indirectly.²¹ Also, it plays a key role in the detection of pancreatic focal lesions since the presence of “duct-penetrating sign” help us rule out the diagnosis of ductal adenocarcinoma.²² Lastly, the MRCP can also be used to evaluate postoperative pancreato-jejunal anastomosis; for the functional assessment of pancreatic transplants; to evaluate the ductal integrity of trauma patients; or for the study of patients with symptomatic elevations of their serum pancreatic enzyme levels. In these patients, the MRCP allows us to significantly increase the diagnosis of the causes of such elevations.²³

Diffusion

The term diffusion refers to the microscopic spontaneous and random move (Brownian motion) of water and other small molecules due to thermal collisions. Diffusion-weighted images (DWI) allow the non-invasive mapping of



Figure 4 Secretin-induced dynamic magnetic resonance cholangiopancreatography (MRCP) in a 57-year-old male with Wirsung' duct disruption after post-trauma splenectomy. Basal MRCP image and image taken 10 min after the administration of secretin – the latter shows the extravasation of pancreatic secretion and the filling of one collection located at the level of the pancreatic tail (red arrow).

such process in *in vivo* biological tissues. The sensitivity of DWI varies depending on the b values used. Higher b values mean heavily diffusion-weighted images. Several factors affect *in vivo* diffusion including the organization and structure of the tissue, its cellularity, and also phenomena of flow and perfusion. Inside the tissues there are different compartments of water distribution: intracellular, extracellular–extravascular and intravascular compartments. Water diffusion in the extracellular–extravascular space is hindered by the presence of cells and the tortuosity of the extracellular–extravascular space, being the main compartment evaluated with the classic diffusion modalities based on monoexponential diffusion-related signal analyses. Thus, tissues or structures where free water molecules are predominant will lose their signal intensity with higher b values; on the contrary, highly-cellular tissues (such as, in general, tumors) and tissues with debris and high protein content (such as abscesses) will keep the integrity of their signal intensity with high b values since the movement of water molecules is restricted here. Lastly, we should remind that in lesions with significant vascularization, the movement of water molecules in the network of microcapillaries creates a process of pseudo-diffusion that will end up modifying the signal intensity in diffusion with low b values, which is the basis for the diffusion model based on the intravoxel incoherent motion (IVIM) technique.

Exponential model of analysis

We can conduct one quantitative analysis of diffusion by estimating the value of the ADC (apparent diffusion coefficient). The ADC represents the exponential decay of signal intensity when increasing diffusion enhancement (b value). With higher diffusion restriction, lower ADC values. In general, there is a significant correlation between ADC values and important biological characteristics such as cellularity; the tumor proliferation index; the tumor grade; or the

presence of necrosis and/or apoptosis. Today, diffusion applies routinely in abdominal MRIs and it provides us with a better detection and characterization of the pancreatic disease.²⁴ It allows the diagnosis of acute pancreatitis with diffusion and a higher sensitivity compared to the CT scan without the administration of contrast.²⁵ Also, diffusion not only allows us to diagnose acute pancreatitis but, thanks to the ADC, it also allows us to score its severity according to the Balthazar severity index.²⁶ In this sense, de Freitas Tertulino et al. determined that ADC values of $1.58 \times 10^{-3} \text{ mm}^2/\text{s}$ identified necrosis with 100% sensitivity and 92.25% specificity.²⁷ However, the main clinical application of diffusion in the context of pancreatitis would be to differentiate pseudo-cysts from abscesses (Fig. 5). The collections infected would show lower ADC values than those of sterile collections.^{28,29}

Another basic application of diffusion in pancreatic images is tumor evaluation. Images play a key role in the detection and characterization of pancreatic cystic masses since around 31% of these lesions can be potentially malignant, being especially significant to differentiate serous from mucinous tumors, and within the latter, to distinguish between cystic mucinous neoplasms (CMN) and intraductal papillary mucinous neoplasms (IPMN) (Fig. 6). Different studies have tried to establish the role played by diffusion in this disease, but the data published so far is contradictory. Thus, Fátima et al. showed that ADC values of $2.4 \times 10^{-3} \text{ s/mm}^2$ differentiate IPMNs from CMNs with 98% sensitivity and 100% specificity. The IPMNs showed systematically higher ADC values compared to CMNs probably due to their communication with Wirsung's duct, which allows greater movement of the content of the lesion.³⁰ On the other hand, the group led by Kang et al. established that diffusion was capable of distinguishing benign from malignant IPMNs while providing information on the degree of aggressiveness based on ADC values.³¹ However, other studies published have provided contradictory findings, meaning that the ADC values

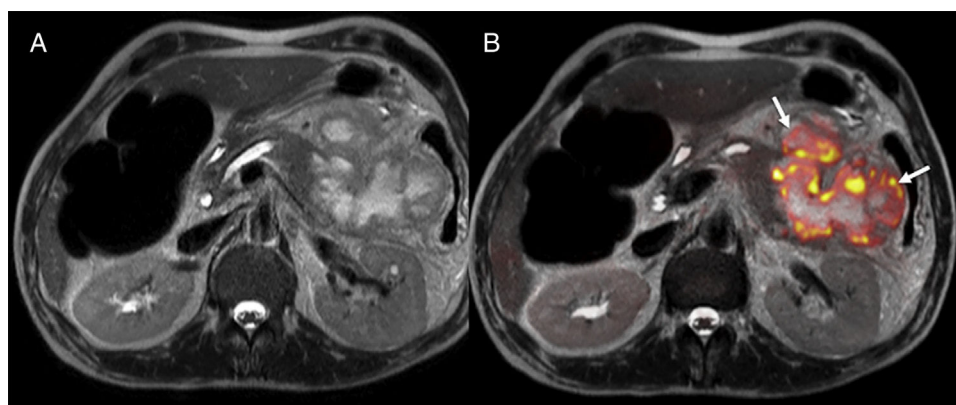


Figure 5 45-year-old patient with necrotizing acute pancreatitis and presence of encapsulated pancreatic and peripancreatic necrosis with signs of infection on the MRI. Axial T2-weighted image (A), diffusion weighted imaging (DWI) in T2 and diffusion imaging with high b values ($b800$) in the color-coded map (B). The fusion of the images shows the restriction of diffusion in the periphery of the collection suggestive of its overinfection (arrows).

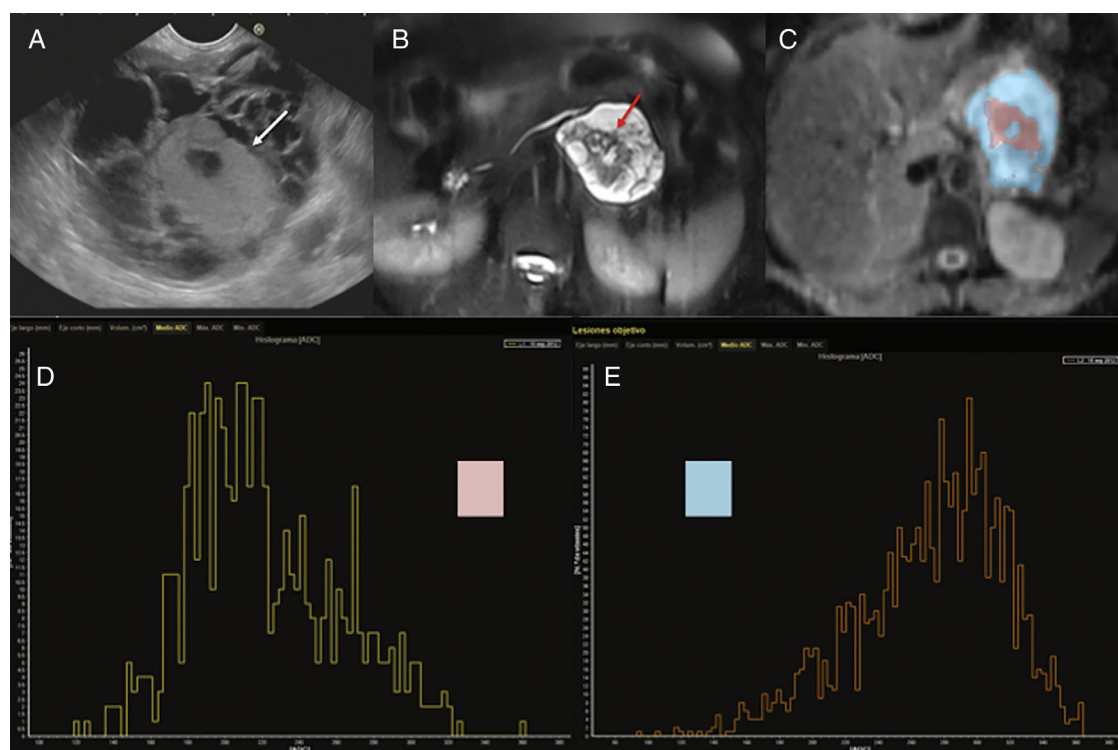


Figure 6 45-year-old female with cystic tumor in the pancreatic tail. Endoscopic ultrasonography (EUS) imaging (A), T2-weighted MRI with fat saturation (B), ADC map with color segmentation of peripheral (blue) and central (pink) portions (C) and histograms corresponding to the ADC values of such portions of the mass (D and E). Both the endoscopic image and the T2-weighted MRI with fat saturation show one cystic mass with a solid central component (white arrows in the EUS image and red arrows in the T2-weighted MRI). The analysis of the ADC map shows the peripheral cystic portion (segmented in blue) with high ADC values in the histogram (E) and an average ADC value of 2.7, while the solid central portion (segmented in pink) shows lower values on the ADC map (D) with an average ADC of 2.1. After the surgery, the anatomopathological diagnosis was mucinous cystadenocarcinoma.

do not help differentiate among different types of pancreatic cystic lesions.^{32,33} For all this, the capacity of individual characterization of one cystic lesion with diffusion would be limited.

Diffusion has also proven highly sensitive and specific with solid tumors when it comes to diagnosing pancreatic

adenocarcinoma improving its detection and staging, and also in the monitoring of therapy. Kartalis et al. and Ichikawa et al. found 92% and 96% sensitivity, respectively, and 97% and 98.6% specificity^{34,35} in its diagnosis – significantly higher values compared to imaging modalities such as the CT scan and the positron emission tomography/computed

tomography (PET)-CT.^{36,37} Compared to the endoscopic ultrasound scan, it is an invasive technique of lower specificity (50%) yet despite its 100% sensitivity.³⁸

Similarly, diffusion can identify small tumor lesions and is particularly useful in the detection of NETs.³⁹ Brenner's group established that by combining T2-weighted images and diffusion-weighted images with high b values it was possible to identify small NETs in almost 100% of the cases.⁴⁰ In this same line, one study that compared the validity of MRIs (including morphological and diffusion sequences) to the validity of PET-CTs with ⁶⁸Ga-DOTANOC found that the capacity of detection of multiparametric MRIs was 92% and superior to that of PET-CTs.⁴¹ With high b values, NETs usually show one marked hypersignal when compared to the gland parenchyma (Fig. 7). However, its ADC values are variables and depend both on the degree of differentiation and on the presence of hemorrhage and/or necrosis. Also, recent studies have described that the ADC is associated with the degree of aggressiveness and the Ki-67; also, higher ADC values have been reported in grade 1 NETs according to the WHO classification of 2011 and lower ADC values have been reported in grade 3 NETs.^{42,43}

On the possibility of characterizing pancreatic lesions, Kartalis et al. showed that malignant pancreatic lesions had lower ADC values compared to benign pancreatic lesions, although overlapping values were found in the different types of malignant lesions.³⁴ There is an extensive medical literature connecting the histopathology of pancreatic adenocarcinoma and ADC values with very diverse and contradictory findings.^{42,44} In this sense, one of the biggest diagnostic challenges of pancreatic imaging is still distinguishing between adenocarcinoma and focal chronic pancreatitis. Different radiological signs such as the duct-penetrating sign or the enhancement peak have been used showing highly variable sensitivities and specificities in different studies.^{22,45} For this reason, Wieggermann et al. evaluated the role played by diffusion and ADC values in the differentiation between focal pancreatitis and adenocarcinoma and confirmed that diffusion and ADC helped distinguish between normal and abnormal pancreatic tissue but there was also ADC value overlapping that would not allow making distinctions between both entities.⁴⁶ One meta-analysis that included 9 studies confirmed 86% and 82% sensitivity and specificity, respectively, when an ADC value of 0.91 was established as the cut-off point.⁴⁷

One of the main advantages of the use of diffusion in pancreatic cancer is the identification of metastatic disease (Fig. 8) since 80% of the cases are unresectable at diagnosis. The findings of one study on metastatic disease in pancreatic cancer showed that diffusion was more sensitive and specific in the detection of hepatic metastases than multidetector CT with contrast with values of 86.7% and 97.5%, respectively *versus* 53.3% and 77.8% for the CT scan.⁴⁸ However, diffusion shows a very limited capability in the assessment of adenopathies.⁴⁴ Diffusion is also a promising tool to assess the response new percutaneous therapies such as cryoablation and/or electroporation and it can also provide prognostic information in patients with locally advanced pancreatic cancer since lower ADC values have been associated with shorter progression-free survival.⁴⁴

Other models of diffusion

Aside from the classic analysis of the diffusion signal, there are other alternative models we can use such as the IVIM (that allows measuring perfusion from the diffusion signal), the diffusion tensor imaging (DTI – that enables the assessment of tissue microstructure), or kurtosis model (that provides information on the heterogeneity and complexity of the tissues). The IVIM model allows us to discriminate two (2) different elements in the drop of signal intensity by increasing the sequence diffusion power. With low b values (between 0 and 100–200 s/mm²), the signal undergoes one quick drop due to the passage of blood through the microvascular network, and with higher b values (above 100–200 s/mm²), the drop of signal intensity is associated with the behavior of water molecule diffusion in the interstitial space regardless of the effects derived from perfusion and with a much more progressive drop (Fig. 9). Through the analysis of perfusion three (3) parameters may be obtained: D^* corresponds to pseudo-diffusion, that is, blood diffusion in the capillary bed; D shows the diffusion coefficient (perfusion-free true diffusion or tissue diffusivity) and perfusion fraction (f) is indicative of the volume of water in the capillary component in relation to the total water volume of the voxel known by some authors as active capillary density. This analytical model would allow us to differentiate patients with pancreatic disease (pancreatitis and different types of tumor) from those with a healthy pancreatic parenchyma, which in turn would be useful when it comes to differentiating adenocarcinomas from NETs.⁴⁹ The studies published to date have also shown significant differences in f between carcinomas and focal pancreatitis.⁵⁰ However, the IVIM does not distinguish focal chronic pancreatitis from pancreatic carcinomas.⁵¹ New applications of the IVIM technique in the pancreas have become more and more popular in the scientific literature. A correlation between the parameters obtained using the IVIM technique (such as D) and the degree of gland fibrosis (a common element both of chronic pancreatitis and adenocarcinomas)^{52,53} and the possible use as a biomarker in the therapeutic monitoring of NETs⁵¹ and autoimmune pancreatitis has been reported.⁵⁴

The DTI technique is based on the fact that water molecule diffusion is one three-dimensional anisotropic phenomenon that is stronger in one direction compared to others, due to different factors such as cell membranes or fibrosis and the duct microstructure so typical of secretory organs like the pancreas. Different studies have shown relatively high values of anisotropy in the normal pancreas with significant changes in patients with cancer or inflammation. Nissan et al. showed significant differences in the degree of anisotropy between healthy patients and those with chronic pancreatitis.⁵⁵

At the moment, the use of the kurtosis model of diffusion is not very popular for pancreatic assessment (Fig. 9). Nevertheless, preliminary findings show that the reliability of diffusion when it comes to differentiating tumor tissues from healthy tissues can improve in patients with pancreatic adenocarcinomas.⁵⁶ Also, Noda et al. said that the kurtosis model may be associated with the levels of glycosylated hemoglobin of diabetic patients.⁵⁷

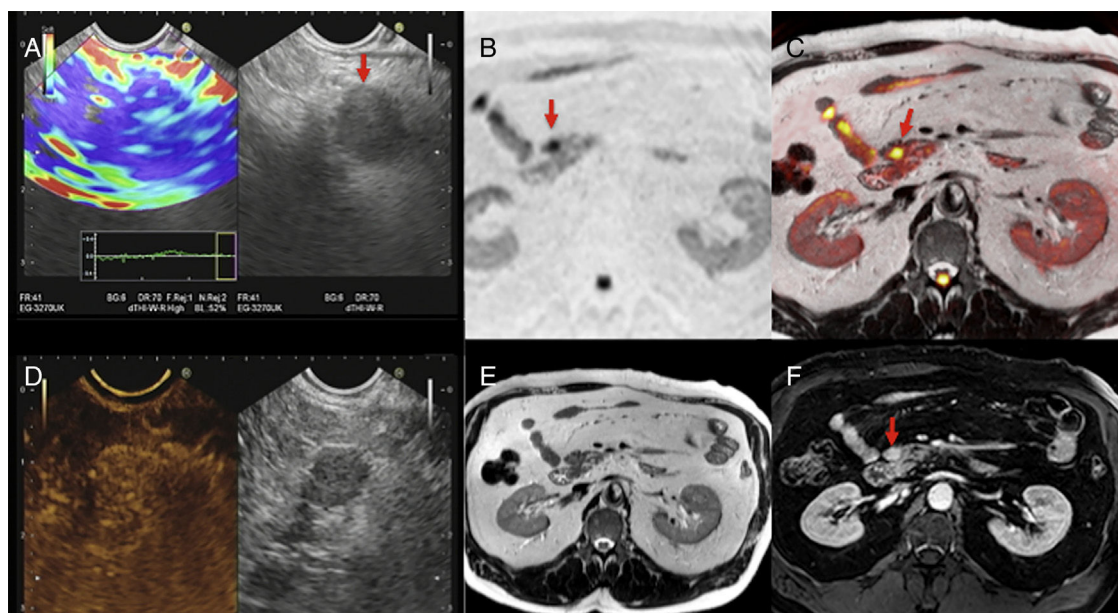


Figure 7 Multimodal image of one pancreatic neuroendocrine tumor. Images of an endoscopic ultrasound with elastography (A), diffusion imaging in $b1000$ with gray-scale inversion (B), fusion of the T2-weighted imaging and the diffusion imaging in $b1000$ in color (C), endoscopic study with ultrasound contrast (D), T2-weighted MRI (E) and T1-weighted MRI with contrast in the portal phase (F). The endoscopic ultrasound scan shows one lesion (red arrow in A) with a homogeneous blue elastographic pattern (common of malignant tumors) and enhancement after the administration of contrast (D). The MRI with diffusion (B) and the fusion imaging color map (T2 + diffusion) (C) clearly show one small tumor in the pancreatic isthmus that looks more enhanced than the parenchyma after the administration of paramagnetic contrast (F) (red arrows).

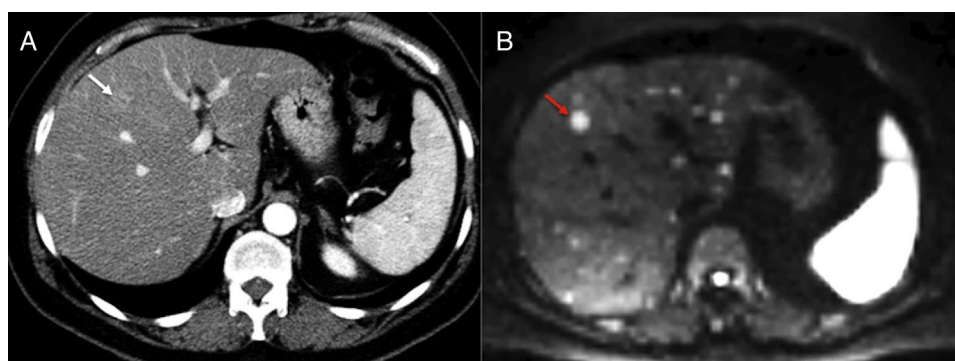


Figure 8 Staging of pancreatic tumors using DWI. Patient operated on one pancreatic neuroendocrine tumor with high levels of chromogranin A during follow-up. The image from the CT scan with contrast in the arterial phase and on the axial plane (A) shows one slightly hypervascular hepatic lesion (white arrow). At the same level of the CT scan, the DWI of the liver with a $b800$ value (B) confirms the existence of this lesion (red arrow) and shows countless hepatic subcentrimetrical lesions with hypersignal in diffusion corresponding to hepatic metastases.

Magnetic resonance perfusion imaging

Multiple MRI imaging modalities can be used to assess pancreatic perfusion, but the most widely used of all are the dynamic perfusion techniques with T1-weighted sequences after the administration of one contrast agent.⁵⁸ The magnetic resonance perfusion imaging (MRPI) assesses the contrast agent kinetics over time by analyzing the passage of the contrast agent through the vascular bed and into the extravascular-extracellular space and providing

information on the nature of the properties of the tissue at the microvascular level. However, quantifying it is much more complex than using the CTP since there is not such a thing as a direct correlation between the tissue signal and the concentration of gadolinium in the tissue; also, the biological correlation of its parameters is much more difficult to draw. This is the reason why the clinical application of the MRPI in the study of pancreatic cancer has been limited (Fig. 10), although pancreatic adenocarcinomas show significantly lower values of K^{trans} , the efflux rate constant (K_{ep}),

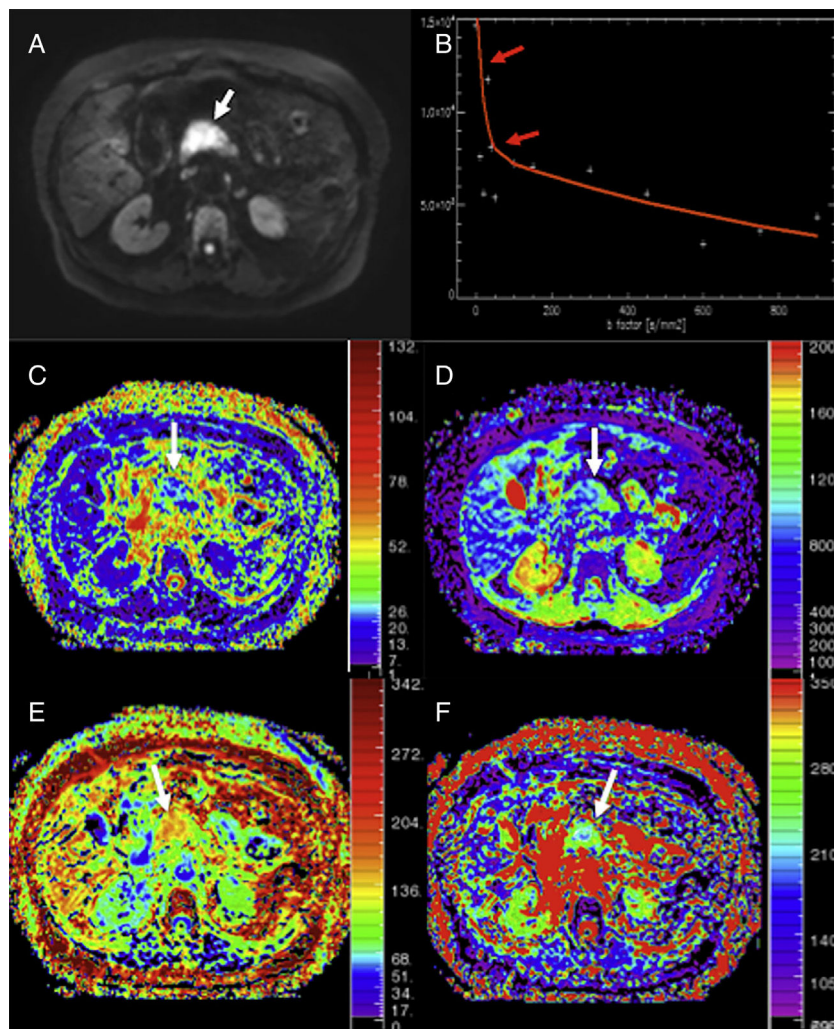


Figure 9 Analysis using monoexponential models of a patient with adenocarcinoma in the pancreatic head (arrows). DWI in $b800$ (A), curve of the drop of signal intensity with higher b values (B), parametric maps obtained using the intravoxel incoherent motion (IVIM) technique of perfusion fraction (C), perfusion-free diffusion (D), kurtosis parametric maps (E), and apparent diffusion (F). The DWI shows the neoplasm (white arrow in A). The tumor shows a marked quick drop of signal intensity in diffusion with higher b values in b values <100 (red arrows in B), suggestive of an important perfusion component and/or pseudo-diffusion in the gland structures of the mass with an average perfusion fraction value (f) of around 25% (C) and low values of perfusion-free diffusion (D^*) (image D). The tumor shows higher kurtosis values (image E) (possibly due to the higher structural complexity of the tumor) and a reduced apparent diffusion or D_k (F) – one parameter used to correct the non-Gaussian behavior of diffusion at high b values.

and the area under the gadolinium concentration-time curve (AUC) compared to adjacent pancreatic tissues.^{59–61} Also, significant differences have been reported in the assessment parameters of perfusion among adenocarcinomas, NETs, and control patients.⁶¹

The MRPI has also been used to assess how NETs respond to therapy.^{62,63} Miyazaki et al. found that a higher hepatic arterial flow is associated with a better response to therapy with octreotide drugs in patients with NETs and hepatic metastasis.⁶³ MRPI techniques have also been used to assess patients with chronic pancreatitis and value overlapping has been confirmed in control patients.⁶⁴

Yet despite their attractive potential to avoid the possible adverse events of contrast agents, the use of other

perfusion techniques that do not require the use of contrast agents such as the arterial spin labeling (ASL) imaging modality is still limited and only used for the assessment of healthy volunteers and diabetic patients.^{65,66}

Magnetic resonance spectroscopy

Magnetic resonance spectroscopies (MRS) allow us to conduct *in vivo* identifications of several molecules involved in the metabolic pathways of physiological or pathological processes.⁶⁷ The use of spectroscopy in the pancreatic gland is limited given its technical difficulties (Fig. 11). Su et al. showed that the main metabolites found in a normal

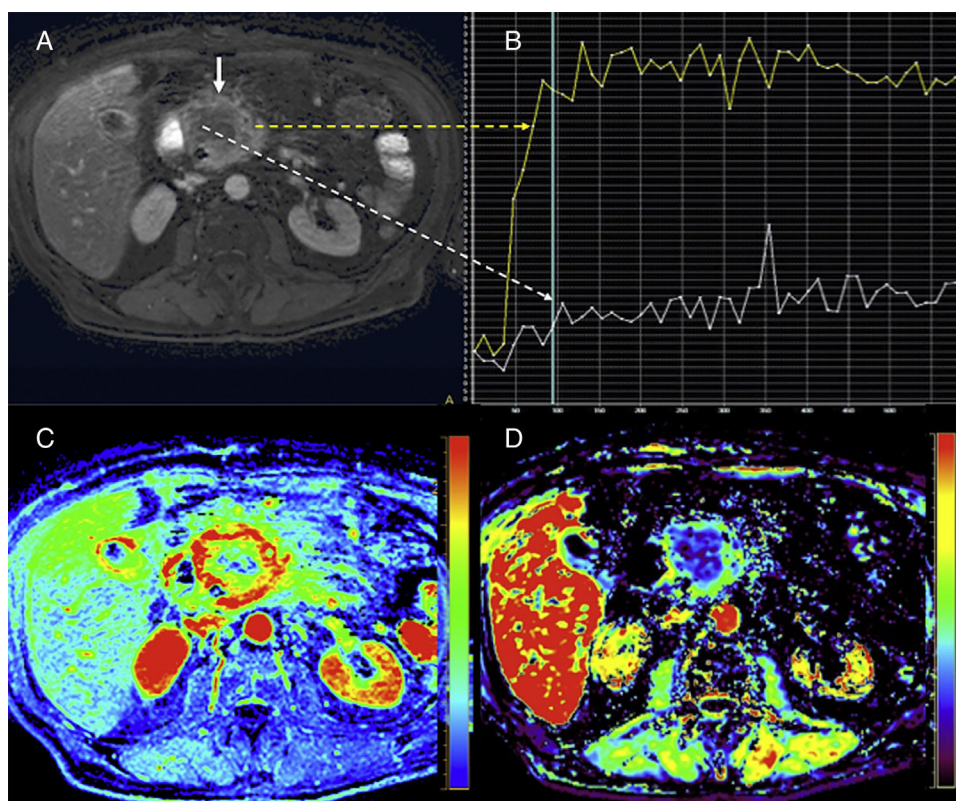


Figure 10 Pancreatic magnetic resonance perfusion imaging study of a patient with head gland pancreatic adenocarcinoma. The dynamic MRI study with contrast (A) conducted shows one large mass with poorly-established edges and extensive areas of central necrosis (white straight solid arrow). The uptake curves (B) show clear differences in the central portion with little enhancement (white curve and dotted arrow) while the more feasible periphery shows type II curve pattern (yellow curve and dotted arrow) with fast enhancement and plateau after the enhancement peak. Also, perfusion allows us to evaluate tissues based on semiquantitative parameters that analyze the characteristics of the enhancement curves such as the area under the curve (AUC) (image C) or quantitative parameters such as the efflux rate constant (K_{ep}) (image D) based on mathematical models that are more difficult to obtain but also much more biologically significant.

pancreatic gland were choline and unsaturated fats.⁶⁸ In general, choline is associated with the metabolism of membrane replacement and unsaturated fats with processes of cell proliferation and growth arrest. Different authors favor the use of the fats found on the spectroscopy as a possible marker of pancreatic cancer. Other authors have reported significant increases of fats in pancreatic cancer.^{69,70} This technique has also been used to distinguish focal chronic pancreatitis from cancer, and significantly lower levels of fats have been found in pancreatitis.⁷¹ Lastly, the MRS can be used for the study of pancreatic metabolic diseases. An increase of the pancreatic fat content determined through the MRS may be associated with insulin resistance in non-obese patients.⁷²

Magnetic resonance relaxometry

A basic part of contrast among tissues provided by the MRI comes from its T1 and T2 characteristics. The alteration of the T1 signal of the pancreas is correlated with the pancreatic exocrine function possibly due to the loss of protein-rich acinar cells and to the fact that they are being replaced by fibrosis. That is why quantifying the T1 relaxation time may provide a quantitative assessment for the diagnosis of pancreatitis.⁷³

In the future, the use of multiple advanced imaging modalities for the assessment of pancreatic disease may provide better assessments of the imaging phenotypes of patients. The combination of multiple data collected from the images including clinical data, genetic, epigenetic, or

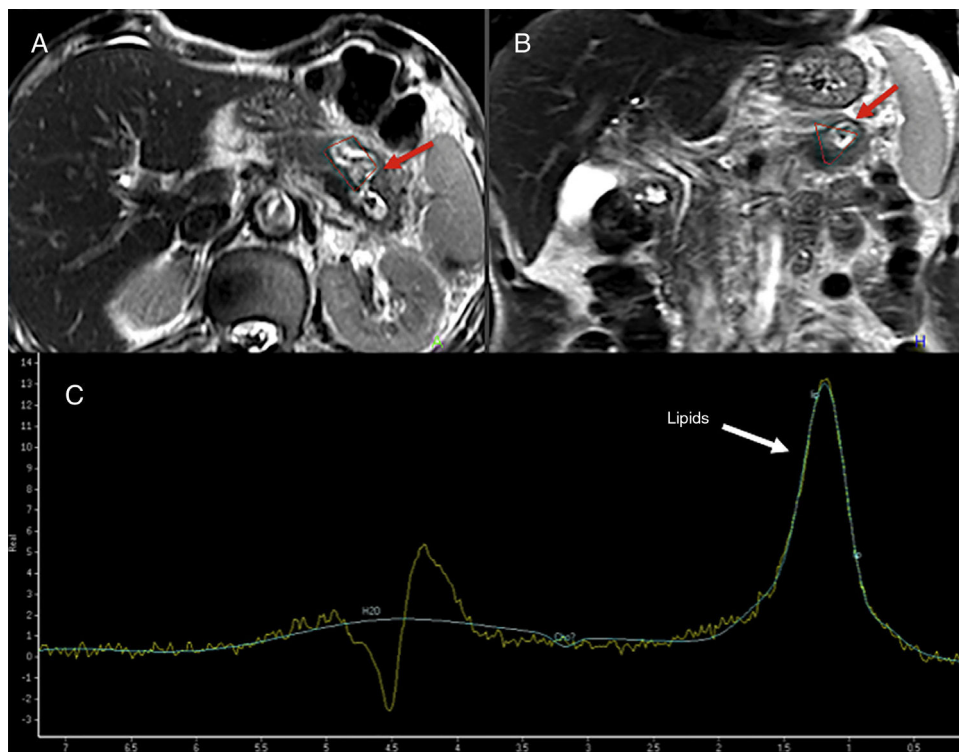


Figure 11 74-year-old-male admitted to the hospital with abdominal pain. The T2-weighted turbo spin-echo sequences on the axial (A) and coronal (B) planes used as a reference to locate the lesion show one 4 cm-cystic mass located in the pancreatic body-tail that looks markedly hyperintense on T2 (red arrows). The spectroscopy with a short echo time (ET) of 35 ms (C) shows fat peak levels at 1.3 ppm possibly suggestive of necrosis. The surgery confirmed the presence of one cavitated lesion with necrohemorrhagic content and epithelial coverage consistent with one mucinous tumor.

proteomic information (the so-called radiomics and radiogenomics) will be key to conduct individual approaches in the management of these patients (personalized medicine) and in the development of imaging biomarkers of the pancreatic disease.^{74,75}

Conclusion

Functional images provide a series of advantages in the assessment of the pancreatic disease that exceed the limitations of anatomical imaging. Today, diffusion is a fundamental imaging modality that has had an impact on the detection and characterization of pancreatic lesions; tumor staging; and therapy response assessment systems. On the other hand, the use of secretin in cholangiographic studies allows us to conduct non-invasive assessments of how the exocrine gland actually works. Lastly, perfusion techniques provide us with an adequate assessment of cancer patients' response to targeted therapies. Nevertheless, a more significant implementation of functional imaging modalities in the clinical practice will require the correct standardization of these techniques.

Authors

1. Manager of the integrity of the study: SBG and RGF.
2. Study idea: SBG, MRD and AL.
3. Study design: SBG, JCV and RFG.

4. Data mining: SBG, MR and RGF.
5. Data analysis and interpretation: SBG, RGF, MR, AL and JCV.
6. Statistical analysis: N.A.
7. Reference: SBG, MR and RGF.
8. Writing: SBG, RGF, MR, AL and JCV.
9. Critical review of the manuscript with intellectually relevant remarks: SBG, RGF, MR, AL and JCV.
10. Approval of final version: SBG, RGF, MR, AL and JCV.

Conflicts of interests

The authors declare no conflicts of interests associated with this article whatsoever.

References

1. Marin D, Nelson RC, Barnhart H, Schindera ST, Ho LM, Jaffe TA, et al. Detection of pancreatic tumors, image quality, and radiation dose during the pancreatic parenchymal phase: effect of a low-tube-voltage, high-tube-current CT technique-preliminary results. *Radiology*. 2010;256:450–9.
2. Macari M, Spieler B, Kim D, Graser A, Megibow AJ, Babb J, et al. Dual-source dual-energy MDCT of pancreatic adenocarcinoma: initial observations with data generated at 80 kVp and at simulated weighted-average 120 kVp. *AJR Am J Roentgenol*. 2010;194:W27–32.
3. Quiney B, Harris A, McLaughlin P, Nicolaou S. Dual-energy CT increases reader confidence in the detection and

- diagnosis of hypoattenuating pancreatic lesions. *Abdom Imaging*. 2015;40:859–64.
4. Yin Q, Zou X, Zai X, Wu Z, Wu Q, Jiang X, et al. Pancreatic ductal adenocarcinoma and chronic mass-forming pancreatitis: differentiation with dual-energy MDCT in spectral imaging mode. *Eur J Radiol*. 2015;84:2470–6.
 5. Clark ZE, Bolus DN, Little MD, Morgan DE. Abdominal rapid-kVp-switching dual-energy MDCT with reduced IV contrast compared to conventional MDCT with standard weight-based IV contrast: an intra-patient comparison. *Abdom Imaging*. 2015;40:852–8.
 6. Wichmann JL, Majenka P, Beeres M, Kromen W, Schulz B, Wesarg S, et al. Single-portal-phase low-tube-voltage dual-energy CT for short-term follow-up of acute pancreatitis: evaluation of CT severity index, interobserver agreement and radiation dose. *Eur Radiol*. 2014;24:2927–35.
 7. Stiller W, Schwarzwaelder CB, Sommer CM, Veloza S, Radeleff BA, Kauczor HU. Dual-energy, standard and low-kVp contrast-enhanced CT-cholangiography: a comparative analysis of image quality and radiation exposure. *Eur J Radiol*. 2012;81:1405–12.
 8. Grözinger G, Grözinger A, Horger M. The role of volume perfusion CT in the diagnosis of pathologies of the pancreas. *Rofo*. 2014;186:1082–93.
 9. Delrue L, Blanckaert P, Mertens D, Cesmeli E, Ceelen WP, Duyck P. Assessment of tumor vascularization in pancreatic adenocarcinoma using 128-slice perfusion computed tomography imaging. *J Comput Assist Tomogr*. 2011;35:434–8.
 10. Delrue L, Blanckaert P, Mertens D, Van Meerbeeck S, Ceelen W, Duyck P. Tissue perfusion in pathologies of the pancreas: assessment using 128-slice computed tomography. *Abdom Imaging*. 2012;37:595–601.
 11. Yadav AK, Sharma R, Kandasamy D, Pradhan RK, Garg PK, Bhalla AS, et al. Perfusion CT – can it resolve the pancreatic carcinoma versus mass forming chronic pancreatitis conundrum? *Pancreatol*. 2016;16:979–87.
 12. d'Assignies G, Couvelard A, Bahrami S, Vullierme MP, Hammel P, Hentic O, et al. Pancreatic endocrine tumors: tumor blood flow assessed with perfusion CT reflects angiogenesis and correlates with prognostic factors. *Radiology*. 2009;250:407–16.
 13. Zhu L, Xue H, Sun H, Wang X, Wu W, Jin Z, et al. Insulinoma detection with MDCT: is there a role for whole-pancreas perfusion? *AJR Am J Roentgenol*. 2017;208:306–14.
 14. D'Onofrio M, Gallotti A, Mantovani W, Crosara S, Manfrin E, Falconi M, et al. Perfusion CT can predict tumoral grading of pancreatic adenocarcinoma. *Eur J Radiol*. 2013;82:227–33.
 15. Park MS, Klotz E, Kim MJ, Song SY, Park SW, Cha SW, et al. Perfusion CT: noninvasive surrogate marker for stratification of pancreatic cancer response to concurrent chemo- and radiation therapy. *Radiology*. 2009;250:110–7.
 16. Yao JC, Phan AT, Hess K, Fogelman D, Jacobs C, Daghoy C, et al. Perfusion computed tomography as functional biomarker in randomized run-in study of bevacizumab and everolimus in well-differentiated neuroendocrine tumors. *Pancreas*. 2015;44:190–7.
 17. Yadav AK, Sharma R, Kandasamy D, Bhalla AS, Gamanagatti S, Srivastava DN, et al. Perfusion CT: can it predict the development of pancreatic necrosis in early stage of severe acute pancreatitis? *Abdom Imaging*. 2015;40:488–99.
 18. Yoshihisa T, Naoki T, Hiroyoshi I, Koizumi K, Koyasu S, Sekimoto M, et al. Early diagnosis of pancreatic necrosis based on perfusion CT to predict the severity of acute pancreatitis. *J Gastroenterol*. 2017;52:1130–9.
 19. Pieńkowska J, Gwoździwicz K, Skrobisz-Balandowska K, Marek I, Kostro J, Szurowska E, et al. Perfusion-CT – can we predict acute pancreatitis outcome within the first 24 hours from the onset of symptoms? *PLoS ONE*. 2016;11:e0146965.
 20. Arikawa S, Uchida M, Kunou Y, Kaida H, Uozumi J, Hayabuchi N, et al. Assessment of chronic pancreatitis: use of whole pancreas perfusion with 256-slice computed tomography. *Pancreas*. 2012;41:535–40.
 21. Cappeliez O, Delhay M, Debiere J, Le Moine O, Metens T, Nicaise N, et al. Chronic pancreatitis: evaluation of pancreatic exocrine function with MR pancreatography after secretin stimulation. *Radiology*. 2000;215:358–64.
 22. Ichikawa T, Sou H, Araki T, Arbab AS, Yoshikawa T, Ishigame K, et al. Duct-penetrating sign at MRCP: usefulness for differentiating inflammatory pancreatic mass from pancreatic carcinomas. *Radiology*. 2001;221:107–16.
 23. Donati F, Boraschi P. Secretin-stimulated MR cholangiopancreatography in the evaluation of asymptomatic patients with non-specific pancreatic hyperenzymemia. *Eur J Radiol*. 2010;75:e38–44.
 24. Barral M, Taouli B, Guio B, Koh DM, Luciani A, Manfredi R, et al. Diffusion-weighted MR imaging of the pancreas: current status and recommendations. *Radiology*. 2015;274:45–63.
 25. Shinya S, Sasaki T, Nakagawa Y, Guiquing Z, Yamamoto F, Yamashita Y. The efficacy of diffusion-weighted imaging for the detection and evaluation of acute pancreatitis. *Hepatogastroenterology*. 2009;56:1407–10.
 26. Yencilek E, Telli S, Tekesin K, Ozgür A, Cakır O, Türkoğlu O, et al. The efficacy of diffusion weighted imaging for detection of acute pancreatitis and comparison of subgroups according to Balthazar classification. *Turk J Gastroenterol*. 2014;25:553–7.
 27. de Freitas Tertulino F, Schraibman V, Ardengh JC, do Espírito-Santo DC, Ajzen SA, Torrez FR, et al. Diffusion-weighted magnetic resonance imaging indicates the severity of acute pancreatitis. *Abdom Imaging*. 2015;40:265–71.
 28. Inan N, Arslan A, Akansel G, Anik Y, Demirci A. Diffusion-weighted imaging in the differential diagnosis of cystic lesions of the pancreas. *AJR Am J Roentgenol*. 2008;191:1115–21.
 29. İslim F, Salik AE, Bayramoglu S, Guven K, Alis H, Turhan AN. Non-invasive detection of infection in acute pancreatic and acute necrotic collections with diffusion-weighted magnetic resonance imaging: preliminary findings. *Abdom Imaging*. 2014;39:472–81.
 30. Fatima Z, Ichikawa T, Motosugi U, Muhi A, Sano K, Sou H, et al. Magnetic resonance diffusion-weighted imaging in the characterization of pancreatic mucinous cystic lesions. *Clin Radiol*. 2011;66:108–11.
 31. Kang KM, Lee JM, Shin CI, Baek JH, Kim SH, Yoon JH, et al. Added value of diffusion-weighted imaging to MR cholangiopancreatography with unenhanced MR imaging for predicting malignancy or invasiveness of intraductal papillary mucinous neoplasm of the pancreas. *J Magn Reson Imaging*. 2013;38:555–63.
 32. Sandrasegaran K, Akisik FM, Patel AA, Rydberg M, Cramer HM, Agaram NP, et al. Diffusion-weighted imaging in characterization of cystic pancreatic lesions. *Clin Radiol*. 2011;66:808–14.
 33. Mottola JC, Sahni VA, Erturk SM, Swanson R, Banks PA, Mortelet KJ. Diffusion-weighted MRI of focal cystic pancreatic lesions at 3.0-Tesla: preliminary results. *Abdom Imaging*. 2012;37:110–7.
 34. Kartalis N, Lindholm TL, Aspelin P, Permert J, Albiin N. Diffusion-weighted magnetic resonance imaging of pancreas tumours. *Eur Radiol*. 2009;19:1981–90.
 35. Ichikawa T, Erturk SM, Motosugi U, Sou H, Iino H, Araki T, et al. High-b value diffusion-weighted MRI for detecting pancreatic adenocarcinoma: preliminary results. *AJR Am J Roentgenol*. 2007;188:409–14.
 36. Fletcher JG, Wiersema MJ, Farrell MA, Fidler JL, Burgart LJ, Koyama T, et al. Pancreatic malignancy: value of arterial, pancreatic, and hepatic phase imaging with multi-detector row CT. *Radiology*. 2003;229:81–90.
 37. Farma JM, Santillan AA, Melis M, Walters J, Belinc D, Chen DT, et al. PET/CT fusion scan enhances CT staging in patients with pancreatic neoplasms. *Ann Surg Oncol*. 2008;15:2465–71.

38. Agarwal B, Abu-Hamda E, Molke KL, Correa AM, Ho L. Endoscopic ultrasound-guided fine needle aspiration and multidetector spiral CT in the diagnosis of pancreatic cancer. *Am J Gastroenterol*. 2004;99:844–50.
39. Park MJ, Kim YK, Choi SY, Rhim H, Lee WJ, Choi D. Pre-operative detection of small pancreatic carcinoma: value of adding diffusion-weighted imaging to conventional MR imaging for improving confidence level. *Radiology*. 2014;273:433–43.
40. Brenner R, Metens T, Bali M, Demetter P, Matos C. Pancreatic neuroendocrine tumor: added value of fusion of T2-weighted imaging and high b-value diffusion-weighted imaging for tumor detection. *Eur J Radiol*. 2012;81:e746–9.
41. Farchione A, Rufini V, Brizi MG, Iacovazzo D, Larghi A, Massara RM, et al. Evaluation of the added value of diffusion-weighted imaging to conventional magnetic resonance imaging in pancreatic neuroendocrine tumors and comparison with 68Ga-DOTANOC positron emission tomography/computed tomography. *Pancreas*. 2016;45:345–54.
42. Wang Y, Chen ZE, Yaghamai V, Nikolaidis P, McCarthy RJ, Merrick L, et al. Diffusion-weighted MR imaging in pancreatic endocrine tumors correlated with histopathologic characteristics. *J Magn Reson Imaging*. 2011;33:1071–9.
43. Kim M, Kang TW, Kim YK, Kim SH, Kwon W, Ha SY, et al. Pancreatic neuroendocrine tumour: correlation of apparent diffusion coefficient or WHO classification with recurrence-free survival. *Eur J Radiol*. 2016;85:680–7.
44. De Robertis R, Tinazzi Martini P, Demozzi E, Dal Corso F, Bassi C, Pederzoli P, et al. Diffusion-weighted imaging of pancreatic cancer. *World J Radiol*. 2015;7:319–28.
45. Momtahan AJ, Balci NC, Alkaade S, Akduman EI, Burton FR. Focal pancreatitis mimicking pancreatic mass: magnetic resonance imaging (MRI)/magnetic resonance cholangiopancreatography (MRCP) findings including diffusion-weighted MRI. *Acta Radiol*. 2008;49:490–7.
46. Wiggemann P, Grützmann R, Weissenböck A, Kamusella P, Dittler DD, Stroszczynski C. Apparent diffusion coefficient measurements of the pancreas, pancreas carcinoma, and mass-forming focal pancreatitis. *Acta Radiol*. 2012;53:135–9.
47. Niu X, Das SK, Bhetuwal A, Xiao Y, Sun F, Zeng L, et al. Value of diffusion-weighted imaging in distinguishing pancreatic carcinoma from mass-forming chronic pancreatitis: a meta-analysis. *Chin Med J (Engl)*. 2014;127:3477–82.
48. Holzapfel K, Reiser-Erkan C, Fingerle AA, Erkan M, Eiber MJ, Rummeny EJ, et al. Comparison of diffusion-weighted MR imaging and multidetector-row CT in the detection of liver metastases in patients operated for pancreatic cancer. *Abdom Imaging*. 2011;36:179–84.
49. Kim B, Lee SS, Sung YS, Cheong H, Byun JH, Kim HJ, et al. Intravoxel incoherent motion diffusion-weighted imaging of the pancreas: characterization of benign and malignant pancreatic pathologies. *J Magn Reson Imaging*. 2017;45:260–9.
50. Kang KM, Lee JM, Yoon JH, Kiefer B, Han JK, Choi BI. Intravoxel incoherent motion diffusion-weighted MR imaging for characterization of focal pancreatic lesions. *Radiology*. 2014;270:444–53.
51. Klauss M, Lemke A, Grünberg K, Simon D, Re TJ, Wente MN, et al. Intravoxel incoherent motion MRI for the differentiation between mass forming chronic pancreatitis and pancreatic carcinoma. *Invest Radiol*. 2011;46:57–63.
52. Hwang EJ, Lee JM, Yoon JH, Kim JH, Han JK, Choi BI, et al. Intravoxel incoherent motion diffusion-weighted imaging of pancreatic neuroendocrine tumors: prediction of the histologic grade using pure diffusion coefficient and tumor size. *Invest Radiol*. 2014;49:396–402.
53. Hecht EM, Liu MZ, Prince MR, Jambawalikar S, Remotti HE, Weisberg SW, et al. Can diffusion-weighted imaging serve as a biomarker of fibrosis in pancreatic adenocarcinoma? *J Magn Reson Imaging*. 2017;46:393–402.
54. Klauf M, Maier-Hein K, Tjaden C, Hackert T, Grenacher L, Stieltjes B. IVIM DW-MRI of autoimmune pancreatitis: therapy monitoring and differentiation from pancreatic cancer. *Eur Radiol*. 2016;26:2099–106.
55. Nissan N, Golan T, Furman-Haran E, Apter S, Inbar Y, Ariche A, et al. Diffusion tensor magnetic resonance imaging of the pancreas. *PLoS ONE*. 2014;9.
56. Kartalis N, Manikis GC, Loizou L, Albiin N, Zöllner FG, Del Chiaro M, et al. Diffusion-weighted MR imaging of pancreatic cancer: a comparison of mono-exponential, bi-exponential and non-Gaussian kurtosis models. *Eur J Radiol Open*. 2016;3:79–85.
57. Noda Y, Kanematsu M, Goshima S, Horikawa Y, Takeda J, Kondo H, et al. Diffusion kurtosis imaging of the pancreas for the assessment of HbA1c levels. *J Magn Reson Imaging*. 2016;43:159–65.
58. Jahng GH, Li KL, Ostergaard L, Calamante F. Perfusion magnetic resonance imaging: a comprehensive update on principles and techniques. *Korean J Radiol*. 2014;15:554–77.
59. Kim H, Arnoletti PJ, Christein J, Heslin MJ, Posey JA 3rd, Pednekar A, et al. Pancreatic adenocarcinoma: a pilot study of quantitative perfusion and diffusion-weighted breath-hold magnetic resonance imaging. *Abdom Imaging*. 2014;39:744–52.
60. Kim JH, Lee JM, Park JH, Kim SC, Joo I, Han JK, et al. Solid pancreatic lesions: characterization by using timing bolus dynamic contrast-enhanced MR imaging assessment: a preliminary study. *Radiology*. 2013;266:185–96.
61. Yao X, Zeng M, Wang H, Sun F, Rao S, Ji Y. Evaluation of pancreatic cancer by multiple breath-hold dynamic contrast-enhanced magnetic resonance imaging at 3.0T. *Eur J Radiol*. 2012;81:e917–22.
62. Armbruster M, Sourbron S, Haug A, Zech CJ, Ingris M, Auernhammer CJ, et al. Evaluation of neuroendocrine liver metastases: a comparison of dynamic contrast-enhanced magnetic resonance imaging and positron emission tomography/computed tomography. *Invest Radiol*. 2014;49:7–14.
63. Miyazaki K, Orton MR, Davidson RL, d'Arcy JA, Lewington V, Koh TS, et al. Neuroendocrine tumor liver metastases: use of dynamic contrast-enhanced MR imaging to monitor and predict radiolabeled octreotide therapy response. *Radiology*. 2012;263:139–48.
64. Coenegrachts K, Van Steenberghe W, De Keyser F, Vanbeckevoort D, Bielen D, Chen F, et al. Dynamic contrast-enhanced MRI of the pancreas: initial results in healthy volunteers and patients with chronic pancreatitis. *J Magn Reson Imaging*. 2004;20:990–7.
65. Schraml C, Schwenzer NF, Martirosian P, Claussen CD, Schick F. Perfusion imaging of the pancreas using an arterial spin labeling technique. *J Magn Reson Imaging*. 2008;28:1459–65.
66. Hirshberg B, Qiu M, Cali AM, Sherwin R, Constable T, Calle RA, et al. Pancreatic perfusion of healthy individuals and type 1 diabetic patients as assessed by magnetic resonance perfusion imaging. *Diabetologia*. 2009;52:1561–5.
67. García-Figueiras R, Baleato-González S, Padhani AR, Oleaga L, Vilanova JC, Luna A, et al. Proton magnetic resonance spectroscopy in oncology: the fingerprints of cancer? *Diagn Interv Radiol*. 2016;22:75–89.
68. Su TH, Jin EH, Shen H, Zhang Y, He W. In vivo proton MRS of normal pancreas metabolites during breath-holding and free-breathing. *Clin Radiol*. 2012;67:633–7.
69. Yao X, Zeng M, Wang H, Fei S, Rao S, Ji Y. Metabolite detection of pancreatic carcinoma by in vivo proton MR spectroscopy at 3T: initial results. *Radiol Med*. 2012;117:780–8.
70. Ma X, Zhao X, Ouyang H, Sun F, Zhang H, Zhou C, et al. The metabolic features of normal pancreas and pancreatic adenocarcinoma: preliminary result of in vivo proton

- magnetic resonance spectroscopy at 3.0T. *J Comput Assist Tomogr.* 2011;35:539–43.
71. Cho SG, Lee DH, Lee KY, Ji H, Lee KH, Ros PR, et al. Differentiation of chronic focal pancreatitis from pancreatic carcinoma by in vivo proton magnetic resonance spectroscopy. *J Comput Assist Tomogr.* 2005;29:163–9.
72. Komada H, Sakaguchi K, Hirota Y, Livingstone R, Klüppelholz B, Keßel K, et al. Pancreatic fat content assessed by ¹H-magnetic resonance spectroscopy is correlated with insulin resistance, but not with insulin secretion, in Japanese subjects with normal glucose tolerance. *J Diabetes Investig.* 2017.
73. Tirkes T, Lin C, Cui E, Deng Y, Territo PR, Sandrasegaran K, et al. Quantitative MR evaluation of chronic pancreatitis: extracellular volume fraction and MR relaxometry. *AJR Am J Roentgenol.* 2018;210:1–10.
74. Permuth JB, Choi J, Balarunathan Y, Kim J, Chen DT, Chen L, et al. Combining radiomic features with a miRNA classifier may improve prediction of malignant pathology for pancreatic intraductal papillary mucinous neoplasms. *Oncotarget.* 2016;7:85785–97.
75. Hanania AN, Bantis LE, Feng Z, Wang H, Tamm EP, Katz MH, et al. Quantitative imaging to evaluate malignant potential of IPMNs. *Oncotarget.* 2016;7:85776–84.